KfK 3416 B
Oktober 1982

Comparison of Thermal Behavior of Different PWR Fuel Rod Simulators for LOCA Experiments

V. Casal, S. Malang, K. Rust
Institut für Reaktorbauelemente
Projekt Nukleare Sicherheit

Kernforschungszentrum Karlsruhe

K E R N F O R S C H U N G S Z E N T R U M K A R L S R U H E

Institut für Reaktorbauelemente
Projekt Nukleare Sicherheit

KfK 3416 B

Comparison of Thermal Behavior of Different PWR Fuel Rod Simulators for LOCA Experiments.

V.Casal, S.Malang, K.Rust

Kernforschungszentrum Karlsruhe GmbH, Karlsruhe

Als Manuskript vervielfältigt
Für diesen Bericht behalten wir uns alle Rechte vor

Kernforschungszentrum Karlsruhe GmbH
ISSN 0303-4003

Vergleich des thermischen Verhaltens verschiedener DWR-Brennstab-simulatoren für Experimente zum Kühlmittelverluststörfall.

Zusammenfassung

Für experimentelle Untersuchungen zum Kühlmittelverluststörfall (LOCA) eines Druckwasserreaktors (PWR) werden als thermische Brennstabsimulatoren elektrische Heizstäbe verwendet.
Um in einem laufenden Untersuchungsprogramm im INSTITUTT FOR ENERGITEKNIKK (OECD-Halden) Heizstäbe aus dem SEMISCALE-Programm durch Heizstäbe von INTERATOM-KfK zu ersetzen, wurde das thermische Verhalten verschiedener Heizstäbe während eines LOCA's verglichen. Die Ergebnisse zeigen, daß SEMISCALE- durch INTERATOM-Heizstäbe ersetzt werden können.

Summary

For experimental investigations of a loss-of-coolant accident (LOCA) of a pressurized water reactor (PWR) electrical heater rods are applied as thermal fuel rod simulators. To substitute heater rods from the SEMISCALE program by INTERATOM-KfK heater rods in a current experimental program at the INSTITUTT FOR ENERGITEKNIKK (OECD-Halden), the thermodynamic behavior of different heater rods during a LOCA were compared. The results show, that SEMISCALE-heater rods can be replaced by those fabricated by INTERATOM.

1. Problem

After a loss-of-coolant accident (LOCA) in a pressurized water reactor (PWR) the fuel cladding temperatures increase due to the stored heat and the decay heat generation. To prevent the cladding temperatures from rising to an unacceptable level, it is necessary to inject sufficient coolant and re-establish adequate heat removal. This task is performed by the emergency core cooling systems.

During the reflood phase steam is generated as water approaches the rods. The steam may reach a velocity at which entrainment and carry over of liquid droplets become possible. The quality of this two-phase flow has a strong influence on the precursory cooling of the hot surface ahead of the quench front and consequently on the peak cladding temperatures.

The internal overpressure of the fuel rods may deform plastically the claddings while being overheated. As a result of the ballooning, the cross-section of the coolant channels may be partly reduced which causes a lower local mass flow rate.

To quantify fuel rod behavior during the sequence of accident events, thermodynamic experiments are being performed by various research institutions. Fuel rod bundles are simulated geometrically and thermally in out-of-pile experiments by electric heaters, so-called fuel rod simulators (FRS).

This study served to compare the thermal behavior of a number of FRS's during the flooding phase. The comparison was made to substitute SEMISCALE FRS's by FRS's manufactured by INTERATOM. These FRS's are provided for flooding experiments to be run by the INSTITUTT FOR ENERGITEKNIKK of Norway (OECD HALDEN REACTOR PROJECT).

The new FRS's are fabricated under a license from KfK. A comparison is made between the SEMISCALE FRS's and four different INTERATOM-FRS's.

2. Fuel Rod Simulator Designs

The FRS's considered have an outer diameter of 10.71 mm. They consist all of an outer cladding and a current conductor with an annular cross-section. The current conductor is insulated electrically against the cladding by a layer of densified boron nitride powder (BN). This BN-layer serves as an electric insulator, a thermal conductor between the current conductor and the cladding tube, and for centering the current conductor in the cladding. The annular current conductors are filled with ceramic material; the SEMISCALE FRS has a BN-filling, the FRS's made by INTERATOM are filled with magnesium oxide (MgO). The design and the dimensions of the FRS's under discussion are shown in cross-section in Figs. 1 to 3. The main characteristics of the heater rods compared are summarized in Table 1. The four FRS's discussed were selected under the following aspects among the numerous FRS's already fabricated by KfK or INTERATOM.

- FRS-No. 1 is equipped with a current conductor already used in an earlier shipment of FRS's by INTERATOM to HALDEN. The rods had balloonable Zircaloy claddings and are being used for emergency cladding experiments on PWR's.

- FRS-No. 2 has an insulating layer, whose thickness is in the normal range (10 to 15 % of the rod diameter).

- FRS-No. 3 and FRS-No. 4 are based on a heater rod used at KfK for sodium boiling experiments. The necessary enlargement of the diameters from 6.0 and 7.6 mm, respectively to 10.71 mm were achieved by a second stainless steel tube swaged on.

3. Data and Methods of Calculation Employed

The decay heat curve used is based on the ANS standard plus a safety margin of 20 %. The rod power amounts to about 24 W/cm at the onset of flooding.

The heat transfer from the rod surface to the coolant as a function of time was taken from a FEBA experiment. The heat transfer coefficient is related to the saturation temperature of steam (144 ^{o}C) at a system pressure of 4.1 bar. In Fig. 4 the decay heat curve and the heat transfer coefficient are plotted versus reflood time. They have been selected so as to simulate, out-of-pile, the behavior of fuel rods.

For the calculation of the transient thermal behavior of the FRS's, the one-dimensional computer code HETRAP /1/ has been used. Depending on the design of the FRS, the rod was modeled by a network consisting of a maximum number of 14 nodes.

The material data required for calculation were taken from reference /2/. Unlike the data indicated there, a density of the boron nitride of 2.1 g/cm^3 and a thermal conductivity of 0.2 (W/cmK) were assumed.

The contact coefficients for heat transfer at the interfaces in the FRS's were selected as follows:

Central filler - current conductor	K = 3 W/cm^{2}K
Current conductor - insulator	K = 25 W/cm^{2}K
Insulator - inner cladding	K = 25 W/cm^{2}K
Inner cladding - outer cladding	K = 3 W/cm^{2}K

For calculating thermal stresses in the claddings of the FRS's a uniaxial stress state was assumed. They were calculated with a modulus of elasticity E = 203,000 (N/mm^2) and a coefficient of thermal expansion α = 16.9 x 10^{-6} (1/K). The biaxial stresses can be determined from the calculated uniaxial ones by taking into

account the Poisson's ratio, ν. For this purpose, the calculated data must be multiplied by the factor $\frac{1}{1-\nu} = 1.43$. The stress rate actually arising in the claddings when the rods are quenched at the end of the flooding phase is difficult to predict. Most probably, the true stress rate is described more appropriately by uniaxial stresses than by biaxial ones, because of the low axial extension of the quench front.

4. Results

The results of the calculation are shown in Fig. 5 to 12. The FRS from the SEMISCALE program is compared with an FRS made by INTERATOM in each case. The cladding temperature, the uniaxial thermal stresses in the cladding, the surface heat flux, and the heat content are plotted each as a function of reflood time. The uniaxial thermal stresses are represented as absolute values. The stresses on the inner phase on the cladding are compressive stresses, those on the outer phase are tensile stresses. The time of 0 seconds on the abscissa of the diagrams marks the onset of flooding. Water enters at the bottom end of the hot rods, the steam generated and the entrained droplets cool the hot surface ahead of the quench front. After 250 seconds, the rod surface was quenched and cooled down towards the coolant temperature (Figs. 5,7,9,11).

The comparability of the different simulators is decisively influenced by the history of the cladding temperatures. During the first 100 seconds after the onset of flooding they rise, then they gradually decrease and drop very rapidly to the coolant temperature after 250 seconds when the quench front arrives (Figs. 5,7,9,11). The temperature rise in the initial phase of flooding can be explained on the basis of the relatively high rod power and the not very efficient heat transfer during the dispersed flow regime (Fig. 4). With increasing flooding time the steam production and the water fraction in the two-phase flow rise; the heat transfer improves while the rod power decreases at the same time. The local clad temperature excursion is terminated.

Comparison of the cladding temperatures shows that FRS's-No. 1 and 2 behave in a completely identical manner as the SEMISCALE FRS. FRS's-No. 3 and 4 have an almost identical transient of cladding temperatures as the SEMISCALE FRS; the differences are only a few K. A factor important for the transient behavior of the cladding temperature is the stored heat. It is seen that FRS-No. 1 has the same behavior of the stored heat as the reference rod (Semiscale). In FRS-No. 2, minimal deviations can be seen. However, FRS's-No. 3 and 4 show approximately 10 % more stored heat than the SEMISCALE FRS.

The heat fluxes of the five FRS's compared with each other are almost identical throughout the whole flooding phase. Only at the final sudden quenching at the end of the flooding phase differences can be perceived which, however, have no longer any influence on the quality of the simulation.

During rewetting at the end of flooding, high thermal stresses occur in the claddings of the heater rods as a result of the high temperature gradients. They are plotted in Figs. 5,7,9,11. In the SEMISCALE rod, the peak compressive stress amounts to 90 N/mm^2. By contrast, FRS's-No. 1 and 2 have only compressive stresses of 55 N/mm^2. In FRS's-No. 3 and 4, peak compressive stresses of 136 and 174 N/mm^2 are calculated. These high values are due to the large wall thickness of the double claddings. These peak stresses occur at a temperature level between 320 and 400 ^{o}C.

To evaluate the stresses, the yield strength (0.2 % offset) of different stainless steels are plotted as a function of temperature in Fig. 13. It is seen that 1.4970 type material can withstand the loads in all cases; however, if materials No. 1.4401 or 1.4541 were used, the permissible stresses were exceeded at least on the inside of FRS-No. 4. The cladding would be permanently deformed. As a consequence, heat transfer at the interfaces in the heater rod will change as the number of tests increases. Changes in the thermal behavior of the FRS's

could not be excluded; tests would no longer be reproducible. For this reason, a cladding material must always be used whose strength ensures accommodation of the thermal stresses in the elastic regime.

5. Evaluation

Calculations show that changes in the internal geometric structure of FRS's practically do not influence their thermal behavior for most of the flooding phase. Even the deviations in cladding temperatures observed in FRS's-No. 3 and 4 can be neglected. This can be explained from the flat temperature profile in the FRS's, which results from the low rod power and the characteristic heat transfer during the flooding phase. At the end of flooding, when heat transfer rises exponentially (Fig. 4), a steeper temperature profile develops in the FRS's. Now changes in the internal structure are reflected in differences in heat flux on the rod surface. Since these differences will have an effect only in the very last seconds of flooding, they are without any importance for flooding experiments. For this reason, all four FRS's offered by INTERATOM as substitutes for the SEMISCALE FRS can be regarded as suitable. However, in case of FRS-No. 4 a high temperature cladding material must be chosen, because of the high thermal stresses.

Since a selection must be made among the FRS's discussed, the authors of this report opt for FRS-No. 2. It offers the best quality of simulation, avoids double claddings, which would entail some uncertainties in the thermal contact between the two tubes and, moreover, the current conductor has a larger diameter, which facilitates electrical connection.

Literature

/1/ S. Malang: HETRAP: A Heat Transfer Analysis Program;
ORNL-TM-4555, (Sept. 74)

/2/ K. Rust, S. Malang, W. Götzmann: PEW
ein FORTRAN-Rechenprogramm zur Bereitstellung physikalischer Eigenschaften von Werkstoffen für LWR-Brennstäbe und deren Simulatoren;
KfK-Ext. 7/76-1 (Dez. 76)

/3/ Materials Properties Table published by
Essener Apparatebau GmbH
4300 Essen-Altenessen, Palmbuschweg 8 - 18

	SEMISCALE FRS	FRS-No. 1	FRS-No. 2	FRS-No. 3	FRS-No. 4
outer sheat					
outer diameter mm	10.71	10.71	10.71	10.71	10.71
inner diameter mm	9.21	8.50	8.50	7.60	6.00
material	SS	SS	SS	SS	SS
inner sheat					
outer diameter mm	9.21	---	---	7.60	6.00
inner diameter mm	8.71	---	---	6.40	4.80
material	SS	---	---	SS	SS
insulator					
outer diameter mm	8.71	8.50	8.50	6.40	4.80
inner diameter mm	5.40	3.50	5.00	5.00	3.40
material	BN	BN	BN	BN	BN
heating element					
outer diameter mm	5.40	3.50	5.00	5.00	3.40
inner diameter mm	3.78	2.90	4.40	4.40	2.80
material	NiCr80 20	NiCr80 20	NiCr80 20	NiCr80 20	NiCr80 20
filler					
outer diameter mm	3.78	2.90	4.40	4.40	2.80
material	MgO	MgO	MgO	MgO	MgO

assumed contact coefficients:

outer sheath - inner sheath = 3 W/(cm×K)
inner sheath - insulator = 25 W/(cm×K)
insulator - heating element = 25 W/(cm×K)
heating element - filler = 3 W/(cm×K)

Table 1: Dimensions and Materials of Fuel Rod Simulators Compared

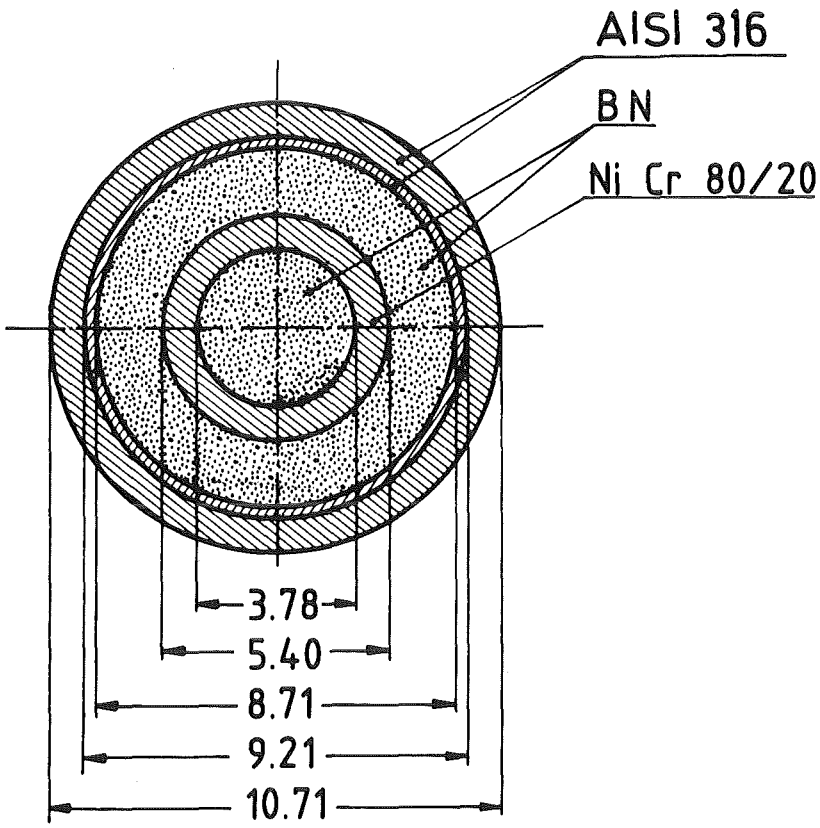

Fig. 1 Cross section of SEMISCALE heater rod

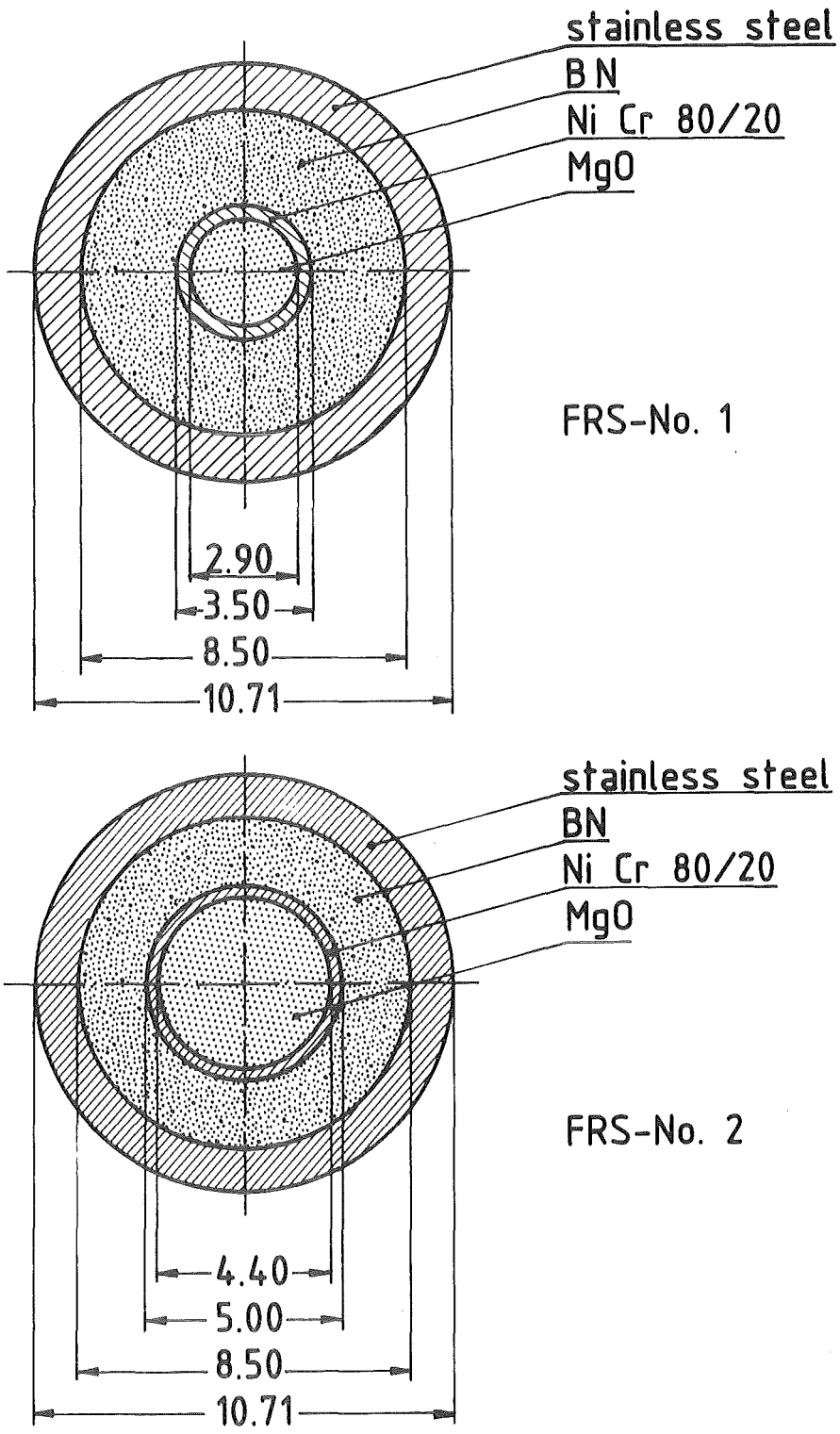

Fig. 2 Cross section of INTERATOM heater rods

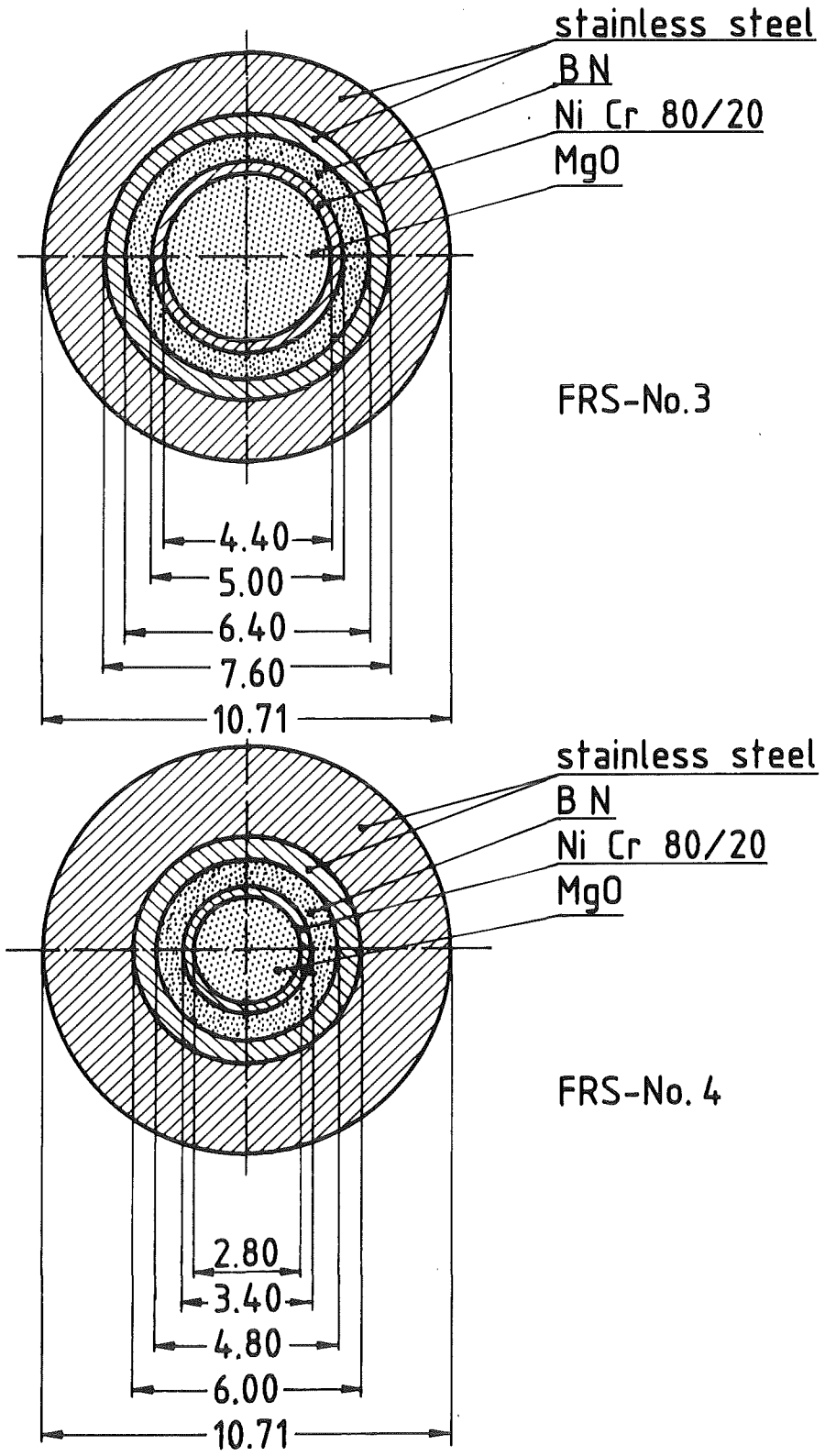

Fig. 3 Cross section of INTERATOM heater rods

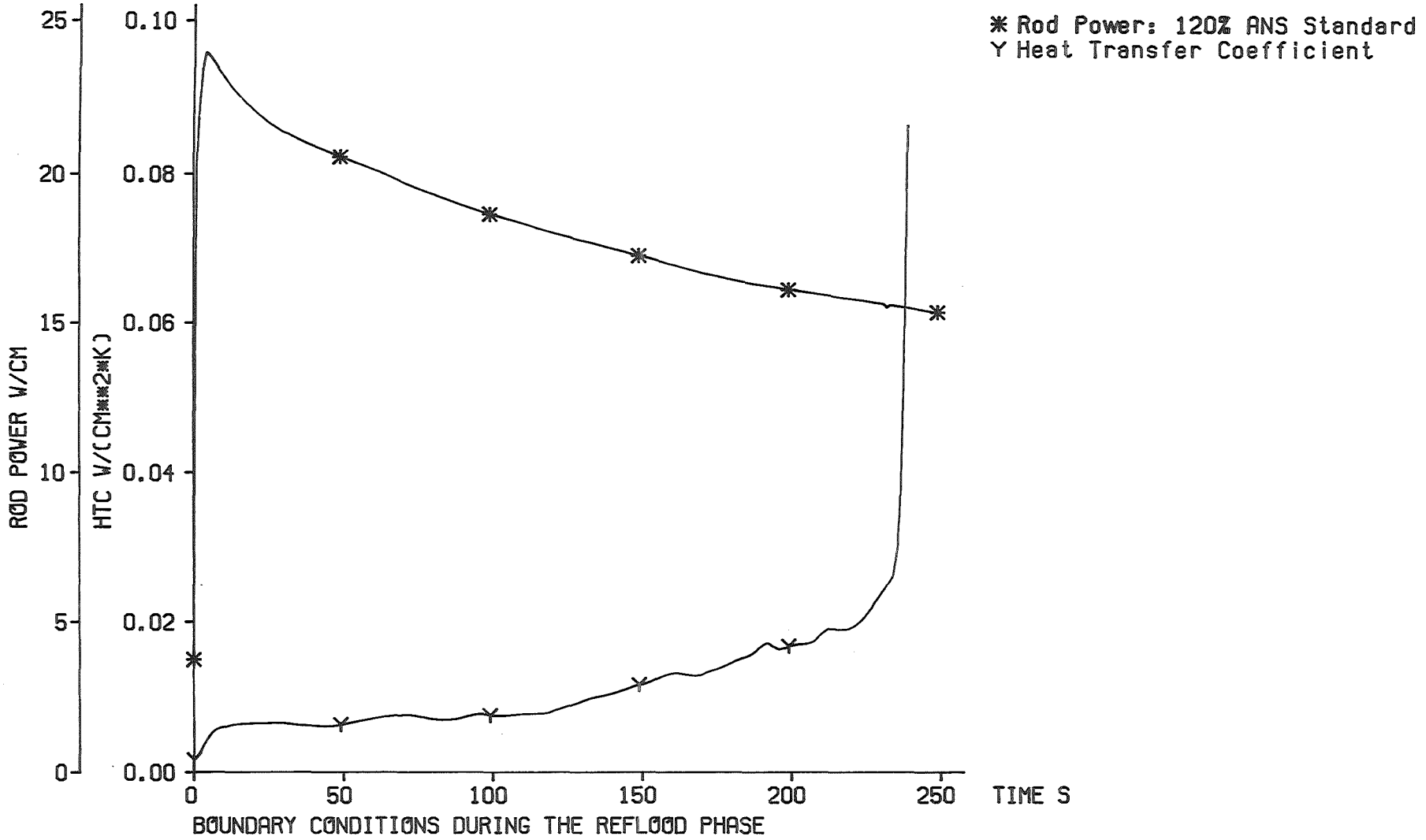

Fig. 4 Thermal Behavior during the Reflood Phase
Rod Power and Heat Transfer Coefficient

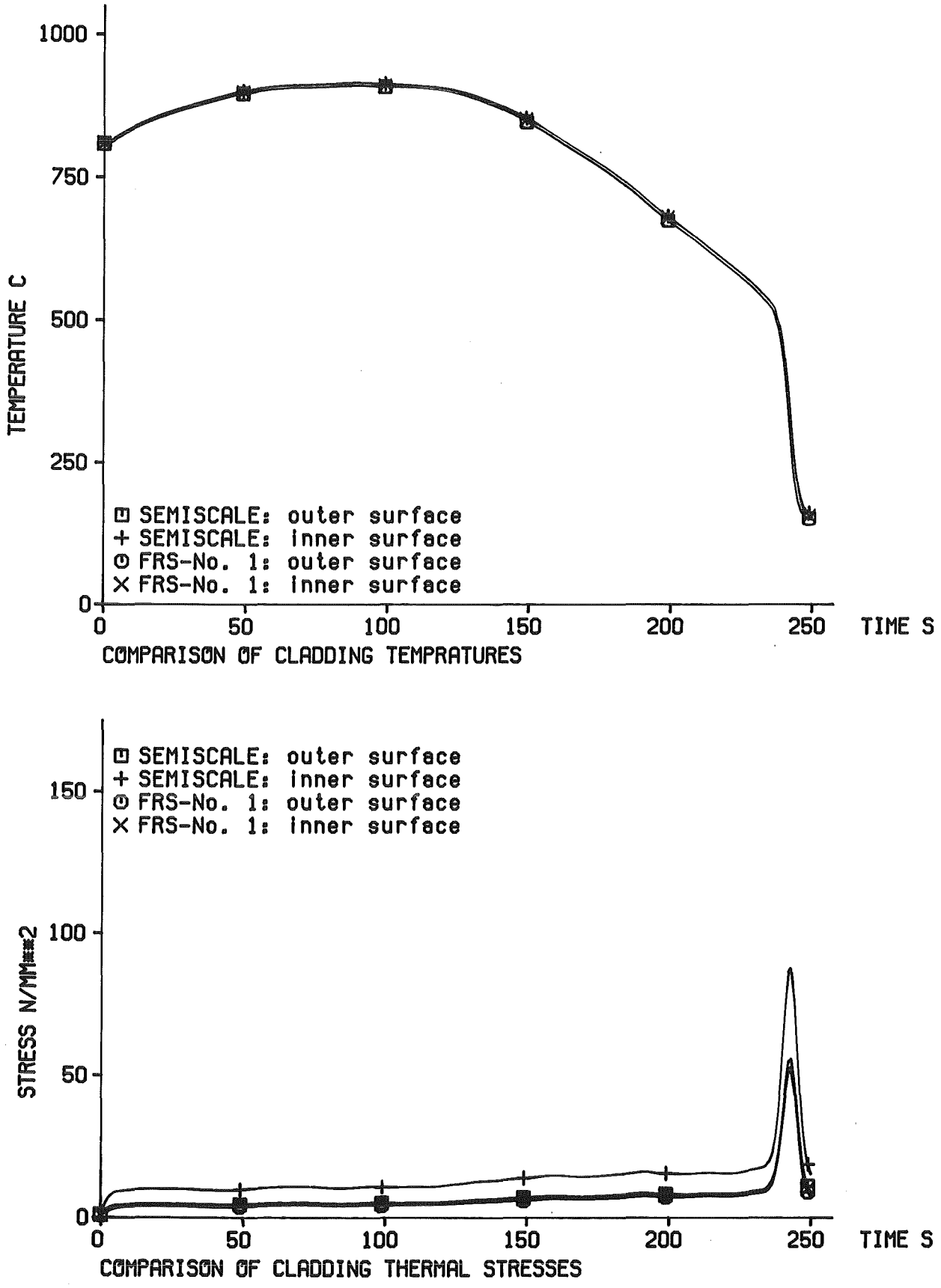

Fig. 5 Thermal Behavior during the Reflood Phase SEMISCALE Heater Rod - INTERATOM FRS-No.1

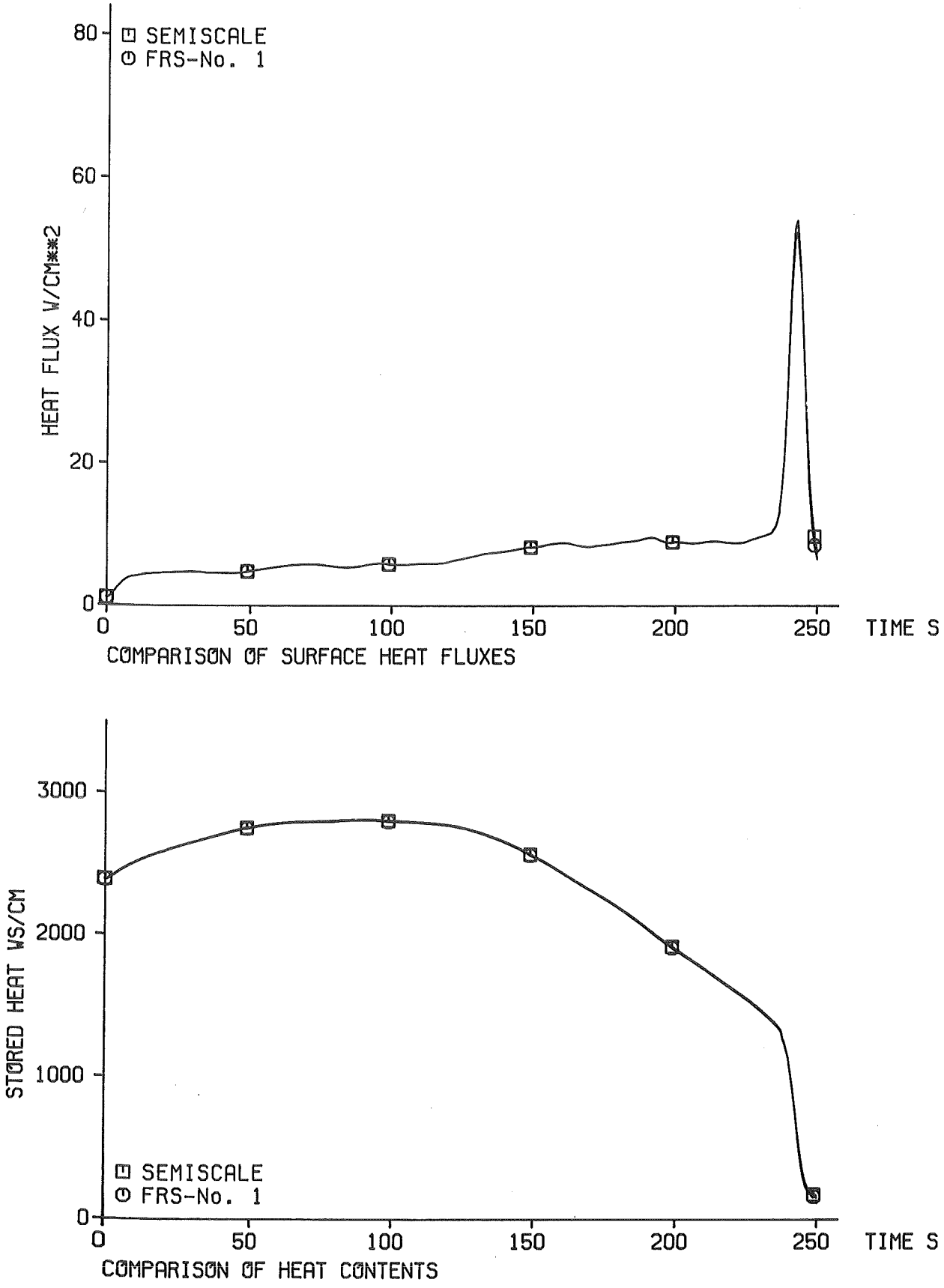

Fig. 6 Thermal Behavior during the Reflood Phase SEMISCALE Heater Rod - INTERATOM FRS-No.1

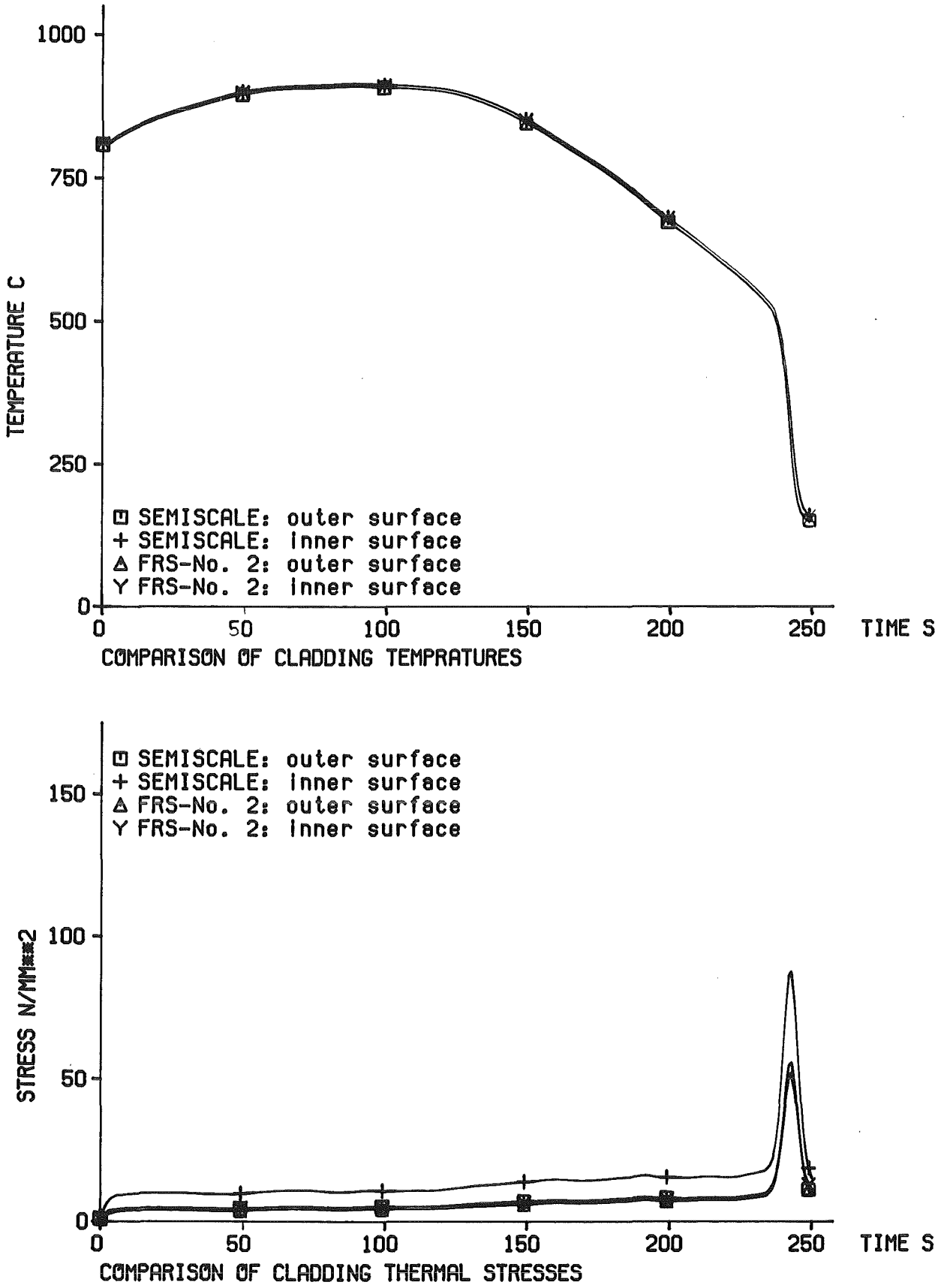

Fig. 7 Thermal Behavior during the Reflood Phase SEMISCALE Heater Rod - INTERATOM FRS-No.2

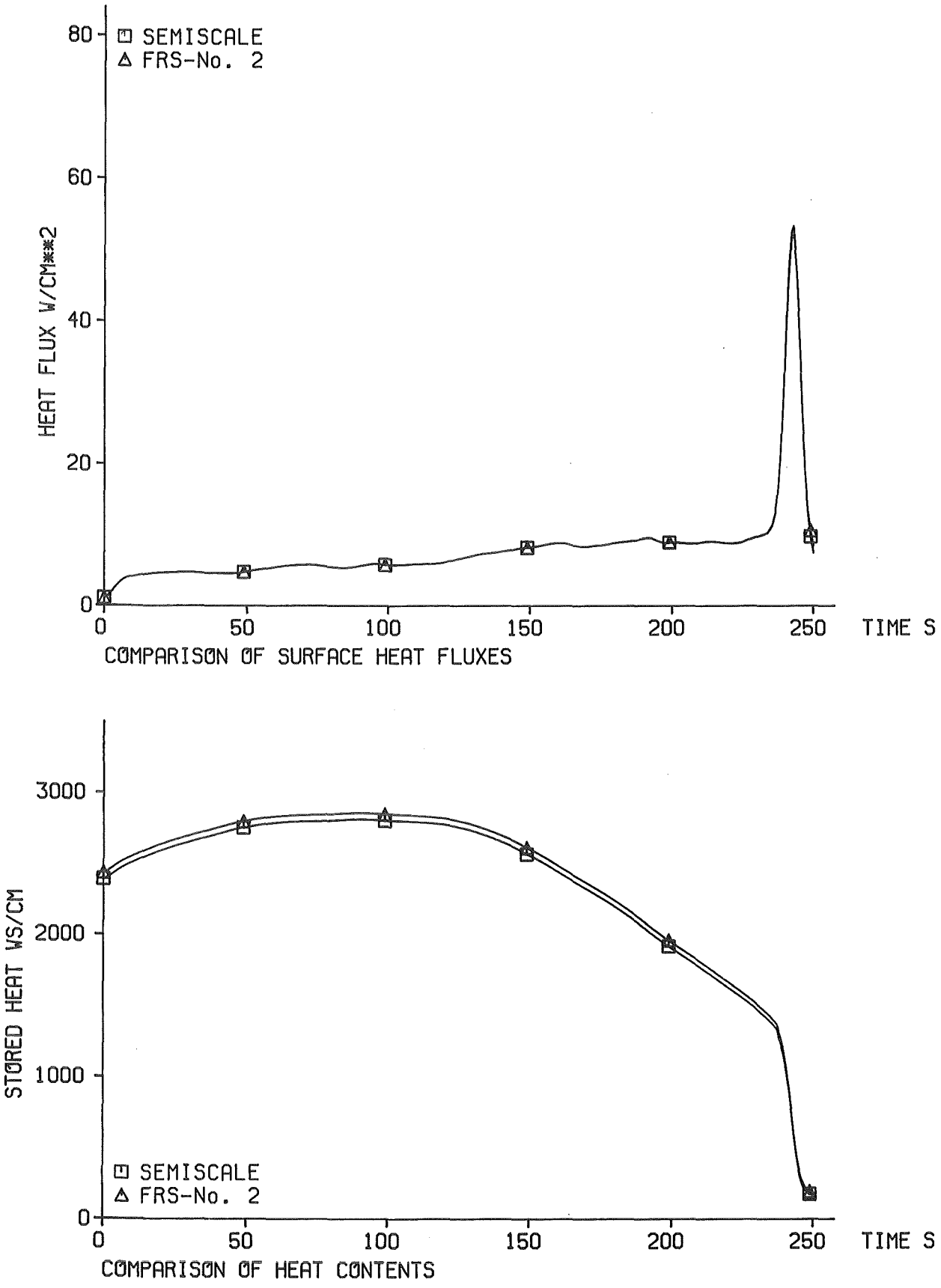

Fig. 8 Thermal Behavior during the Reflood Phase SEMISCALE Heater Rod - INTERATOM FRS-No.2

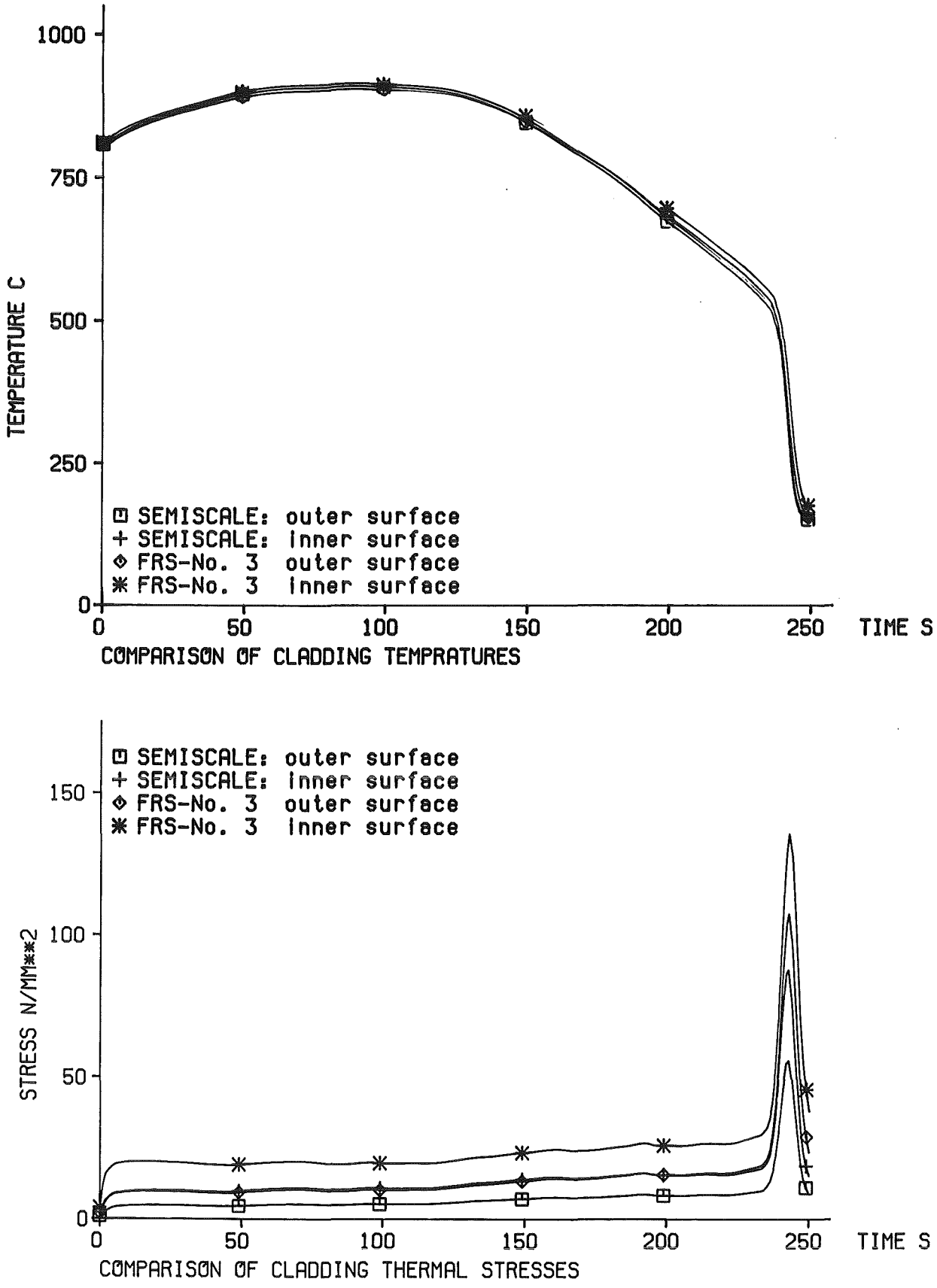

Fig. 9 Thermal Behavior during the Reflood Phase SEMISCALE Heater Rod - INTERATOM FRS-No.3

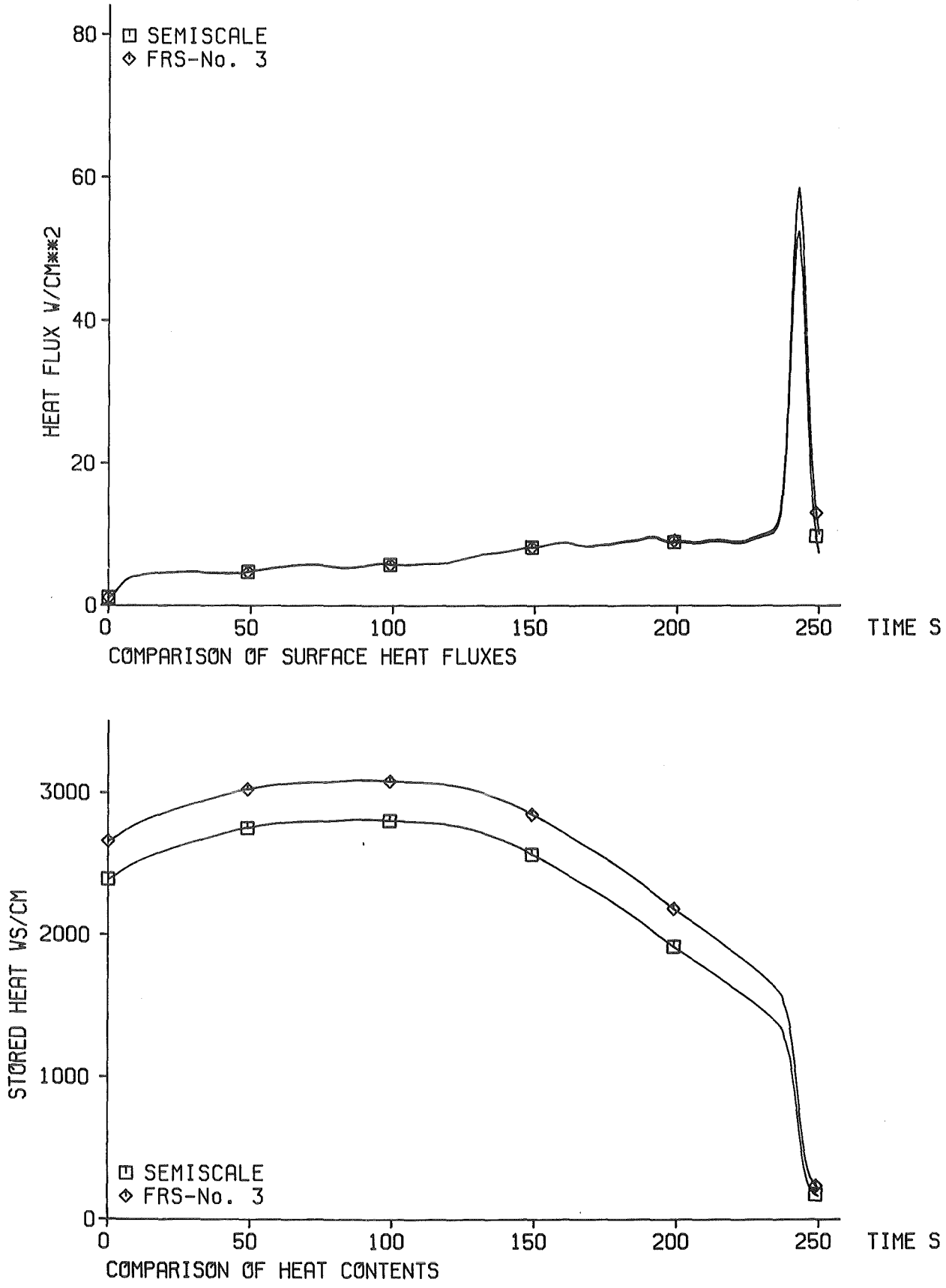

Fig.10 Thermal Behavior during the Reflood Phase SEMISCALE Heater Rod - INTERATOM FRS-No.3

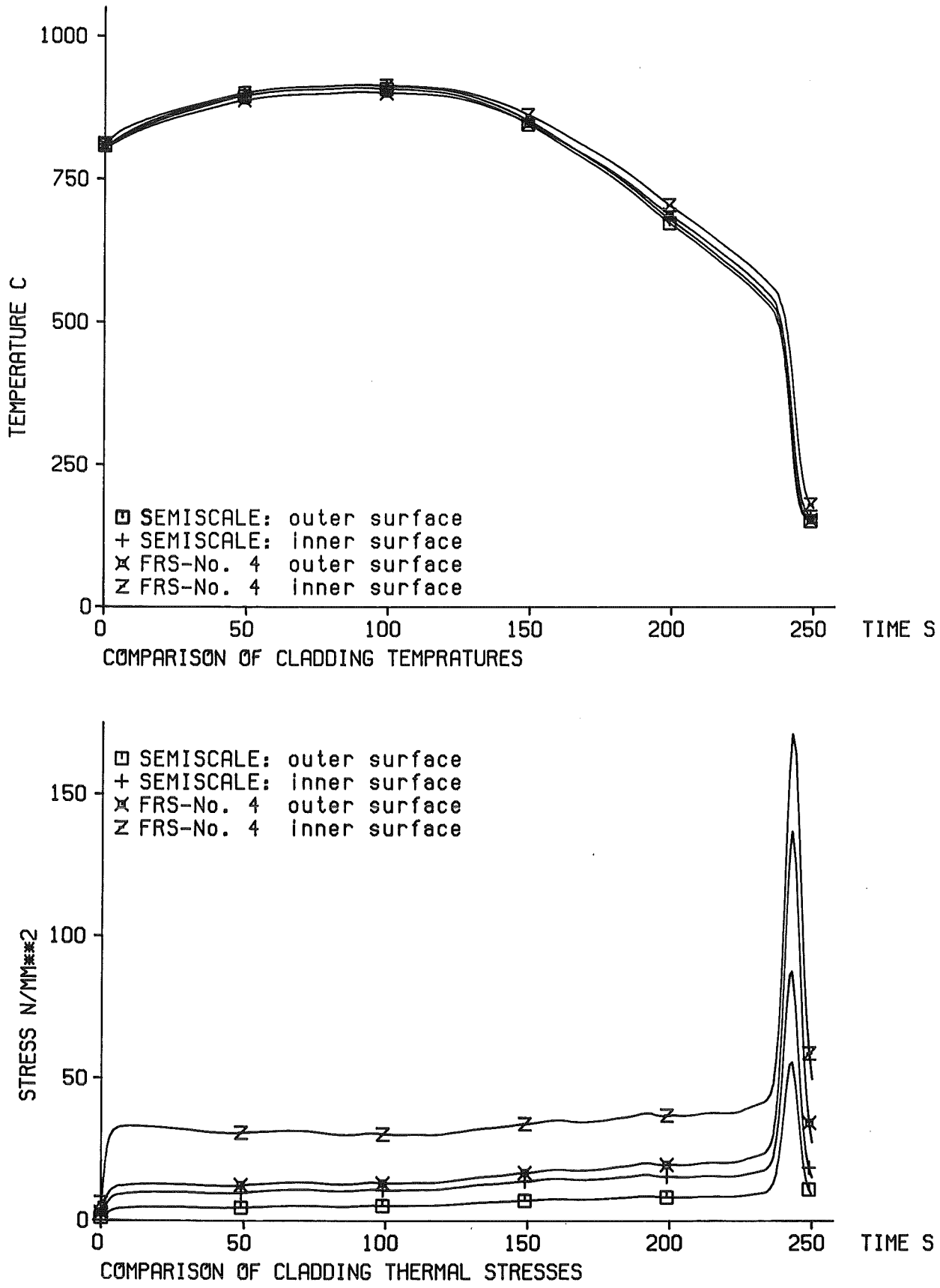

Fig.11 Thermal Behavior during the Reflood Phase SEMISCALE Heater Rod - INTERATOM FRS-No.4

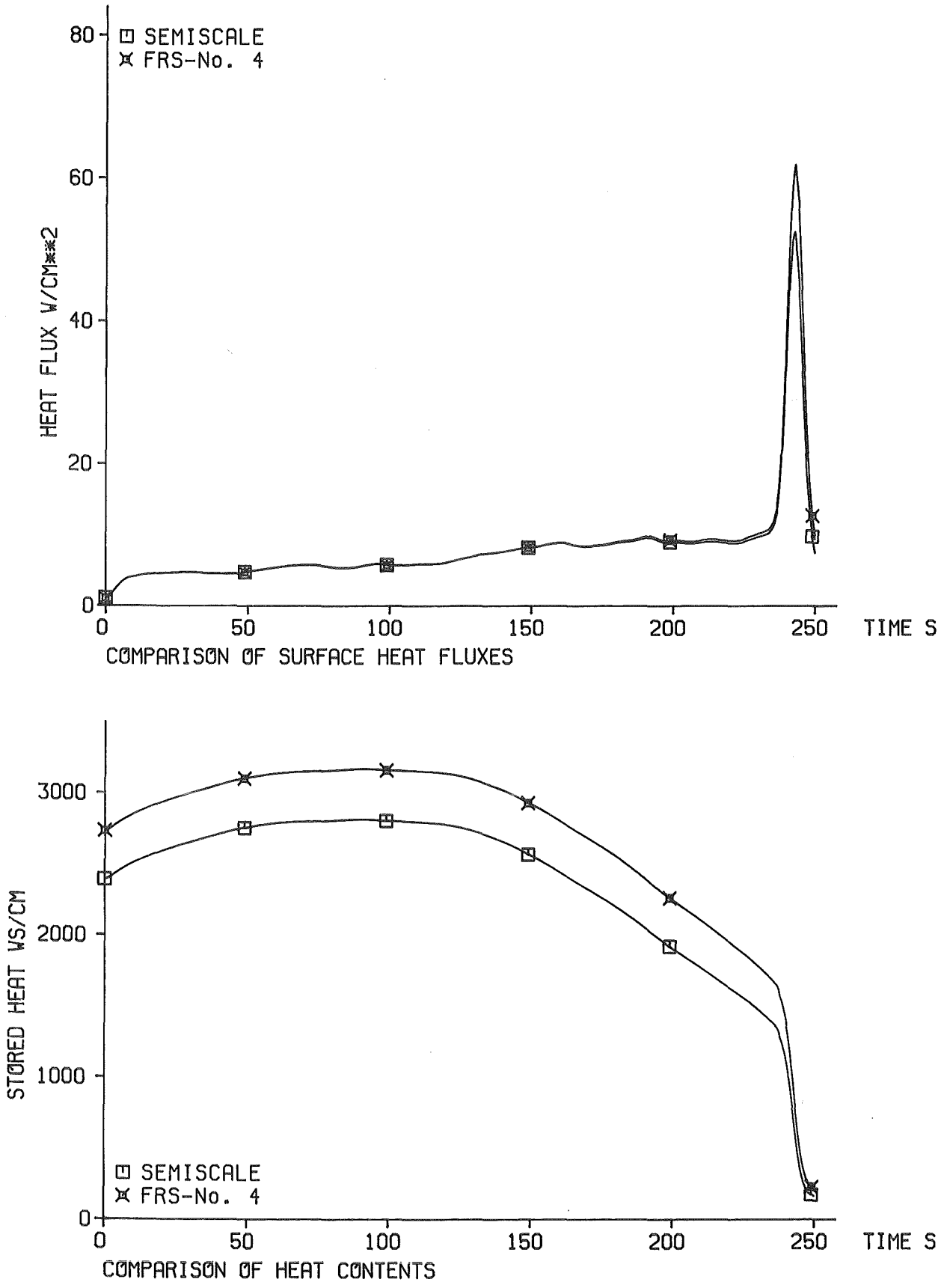

Fig.12 Thermal Behavior during the Reflood Phase SEMISCALE Heater Rod - INTERATOM FRS-No.4

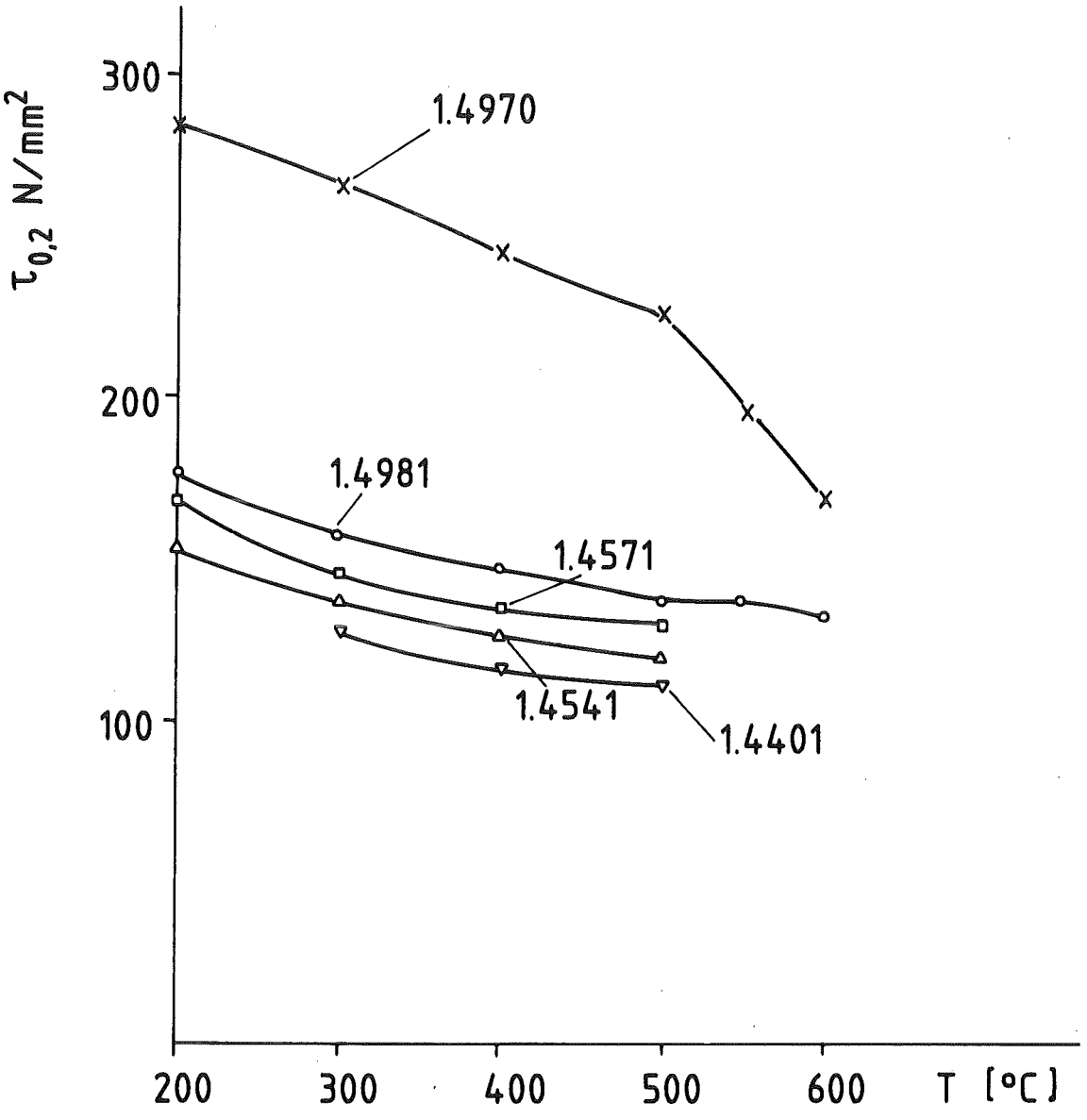

Fig.13 Load with permanent elongation smaller 0,2% ($\tau_{0,2}$) as a function of temperature (T) for different materials /3/